CLINICAL RESEARCH

e-ISSN 1643-3750
© Med Sci Monit, 2026; 32: e952904
DOI: 10.12659/MSM.952904

Received: 2026.01.23
Accepted: 2026.05.15
Available online: 2026.06.07
Published: 2026.XX.XX

Computed Tomography and Plasma Proteomics for Early Discrimination of Post-Pancreatitis Diabetes Mellitus

Authors' Contribution:
Study Design A
Data Collection B
Statistical Analysis C
Data Interpretation D
Manuscript Preparation E
Literature Search F
Funds Collection G

ACEG 1,2 Ran Hu*
ACE 3 Xiao Zeng*
AEG 1 Gangjing Li
AEG 1 Jin Ma
AEG 1 Huiping Yang
B 4 Fang Jiang
CE 5 Zenghui Li
AD 3 Xiaoming Zhang
AD 1 Hua Yang

1 Department of Radiology, Chongqing Hospital of Traditional Chinese Medicine (The First Affiliated Hospital of Chongqing University of Chinese Medicine), Chongqing, PR China
2 Department of Ultrasound, The Second Affiliated Hospital of Chongqing Medical University, Chongqing, PR China
3 Medical Imaging Key Laboratory of Sichuan Province, Department of Radiology, Affiliated Hospital of North Sichuan Medical College, Nanchong, Sichuan, PR China
4 Department of Gastroenterology, Affiliated Hospital of North Sichuan Medical College, Nanchong, Sichuan, PR China
5 Department of Radiology, Langzhong Hospital of TCM, Langzhong, Sichuan, PR China

* Ran Hu and Xiao Zeng made equal contributions to this work

Corresponding Authors: Zenghui Li, Department of Radiology, Langzhong Hospital of T.C.M, No. 33 Zhangfei Road, Langzhong, Sichuan 637400, PR China, Phone: +86-13550585165, e-mail: l_izenghui@163.com; Xiaoming Zhang, Medical Imaging Key Laboratory of Sichuan Province, Department of Radiology, Affiliated Hospital of North Sichuan Medical College; 1 South Maoyuan Street, Nanchong, Sichuan 637001, PR China, Phone: +86-13808271001, e-mail: zhangxm@nsmc.edu.cn; Hua Yang, Department of Radiology, Chongqing Hospital of Traditional Chinese Medicine (The First Affiliated Hospital of Chongqing University of Chinese Medicine); No. 6; Panxi 7th Road, Jiangbei District, Chongqing 400021, PR China, Phone: +86-13527547568, e-mail: 13527547568@163.com

Financial support: This work was supported by the Scientific and Technological Research Program of the Chongqing Municipal Education Commission [grant number KJQN202415136], and the Natural Science Foundation of Chongqing, China [grant numbers CSTB2025NSCQ-GPX1092 and CSTB2025NSCQ-GPX0325]

Conflict of interest: None declared

Background: There is a lack of effective predictive methods for post-pancreatitis diabetes mellitus (PPDM-A) in clinical practice. This exploratory study aimed to identify candidate computed tomography (CT) and plasma proteomic features associated with subsequent PPDM-A and to assess their preliminary discriminatory performance.

Material/Methods: This retrospective single-center study compared CT imaging features and clinical data between post-pancreatitis normal glucose (PPNG-A, n = 10) and PPDM-A (n = 9) groups. Differential plasma protein expression was analyzed using proteomics. Correlations between CT features and protein features in patients with PPDM-A were also assessed.

Results: The PPDM-A group showed higher incidences of pancreatic necrosis and elevated plasma complement factor I (CFI) levels compared with the PPNG-A group. Plasma coagulation factor XII (F12) and immunoglobulin heavy chain (IgH) levels were significantly decreased in the PPDM-A group. Enzyme-linked immunosorbent assay findings validated CFI; F12 and IgH remain proteomics-derived candidate markers. The combined 3-index model achieved an area under the curve of 0.989 for PPDM-A discrimination in the same discovery cohort. CFI was positively correlated with pancreatic necrosis ($P = 0.02$, R = 0.527).

Conclusions: Plasma CFI, F12, and IgH demonstrated potential predictive value for PPDM-A and may help identify at-risk patients. CFI and F12 were significantly correlated with pancreatic necrosis, suggesting a link between plasma molecular markers and imaging manifestations of PPDM-A. These exploratory findings provide a preliminary experimental basis for early discrimination of PPDM-A. Clinical utility requires confirmation in multicenter studies with larger sample sizes and both internal and external validation.

Keywords: pancreatitis • diabetes mellitus • computed tomography • proteomics

Full-text PDF: https://www.medscimonit.com/abstract/index/idArt/952904

Indexed in: [Current Contents/Clinical Medicine] [SCI Expanded] [ISI Alerting System] [ISI Journals Master List] [Index Medicus/MEDLINE] [EMBASE/Excerpta Medica] [Chemical Abstracts/CAS]

Introduction

In recent years, there has been an increase in the morbidity of post-pancreatitis diabetes mellitus (PPDM-A), which is characterized by strong dependence on insulin therapy, frequent and diverse complications, and an overall poor prognosis [1-3]. However, the exact pathogenesis of PPDM-A remains incompletely understood; targeted, effective therapeutic strategies and drugs are absent in clinical practice [4-7]. Therefore, further investigation of the pathogenesis of PPDM-A and identification of predictive indicators are important to improve clinical diagnosis and treatment.

Previous studies generally reported that PPDM-A is primarily triggered by pancreatic β-cell necrosis [8-10]. When extensive pancreatic necrosis occurs, β cells are severely damaged, leading to insufficient insulin secretion and subsequent diabetes mellitus. PPDM-A can also occur in patients with acute pancreatitis in the absence of pancreatic necrosis [11]. In these cases, β-cell damage is relatively mild, and insulin deficiency is not the direct cause of diabetes mellitus, suggesting that PPDM-A pathogenesis is more complex and not limited to β-cell destruction. Specifically, the nuclear factor-κB (NF-κB) signaling pathway, which mediates amplification of pancreatic inflammation [12], and the calcium signaling pathway, which induces early acinar cell injury [13], have been implicated in acute pancreatitis. Additionally, complement-coagulation cascades have been associated with pancreatic inflammation and necrosis [14], whereas IgH-related immune dysregulation may represent a potential contributor to PPDM-A [15].

Due to its high-throughput capacity, proteomics technology can detect expression changes in thousands of molecules simultaneously, comprehensively characterize biological processes, accurately identify key molecules in complex phenotypes or molecular backgrounds, and provide insights to guide subsequent studies [16]. In pancreatic disease research, proteomic analysis has substantially advanced understanding of pathogenesis mechanisms by facilitating the discovery of specific biomarkers and revealing alterations in signaling pathways. Thus far, proteomics has been widely utilized in studies of acute pancreatitis [17,18]. Using proteomics and genomics to analyze altered serum complement components in necrotizing acute pancreatitis, researchers have confirmed a critical role for complement-coagulation cascades in inflammation and pancreatic necrosis [14]. Furthermore, urine proteomics identified elastase 2A as a potential diagnostic marker for pediatric acute pancreatitis [19]. Building on these findings, we used data-independent acquisition (DIA) proteomics to screen for potential predictive indicators of PPDM-A, with a focus on pathways previously implicated in disease pathogenesis. Accordingly, we applied proteomic methods to identify differentially expressed plasma proteins at admission in patients with post-pancreatitis normal glucose (PPNG-A) or PPDM-A, with the goal of identifying predictive protein markers and establishing a discriminatory model for PPDM-A.

As a commonly used imaging modality in acute abdominal conditions, computed tomography (CT) has broad clinical applications in the early diagnosis of acute pancreatitis [14]. In this exploratory, hypothesis-generating study, we aimed to identify candidate admission CT features and plasma proteins associated with subsequent PPDM-A, then assess their predictive performance. We analyzed admission CT images from patients with PPNG-A or PPDM-A, including CT clinical scores such as the revised Atlanta classification (RAC), extrapancreatic inflammation on CT (EPIC), etiology, and CT severity index (CTSI). Differential imaging features were identified, and their correlations with protein markers were analyzed to further elucidate imaging characteristics of PPDM-A at the molecular level.

Material and Methods

Research Design, Participants, and Imaging

Patients with acute pancreatitis hospitalized at the Affiliated Hospital of North Sichuan Medical College between October 2023 and June 2024 were included. Based on medical record review and/or telephone interviews [20], patients with acute pancreatitis were categorized into PPNG-A and PPDM-A groups.

The diagnosis of acute pancreatitis was established according to the 2012 Atlanta consensus criteria [21], requiring at least 2 of the following 3 manifestations: (1) typical epigastric abdominal pain consistent with acute pancreatitis; (2) serum amylase or lipase levels elevated to at least 3 times the upper limit of the normal reference range; and (3) imaging findings characteristic of acute pancreatitis. A diagnosis of diabetes mellitus was confirmed if any 1 of the following criteria was met [22]: (1) fasting plasma glucose of at least 126 mg/dL (7.0 mmol/L); (2) 2-h postprandial plasma glucose of at least 11.1 mmol/L after a 75-g oral glucose tolerance test; (3) random plasma glucose of at least 200 mg/dL (11.1 mmol/L) accompanied by classic hyperglycemic symptoms; or (4) glycated hemoglobin (HbA1c) of at least 6.5% (48 mmol/mol).

The inclusion and exclusion criteria for the PPDM-A cohort were predefined. Inclusion criteria were: (1) new-onset diabetes mellitus diagnosed more than 90 days after the initial acute pancreatitis episode, and hyperglycemia occurring within 90 days was classified as stress-induced hyperglycemia [23-25]; (2) contrast-enhanced computed tomography of the upper abdomen performed within 7 days of acute pancreatitis symptom onset; and (3) inpatient admission at acute pancreatitis onset. The minimum follow-up duration was documented, and

Indexed in: [Current Contents/Clinical Medicine] [SCI Expanded] [ISI Alerting System] [ISI Journals Master List] [Index Medicus/MEDLINE] [EMBASE/Excerpta Medica] [Chemical Abstracts/CAS]

the mean follow-up period was reported with corresponding measures of dispersion. Exclusion criteria were: (1) pre-existing diabetes mellitus; (2) in-hospital hyperglycemia during the acute acute pancreatitis episode; (3) persistent hyperglycemia within 90 days after hospital discharge; (4) acute exacerbation of underlying chronic pancreatitis; (5) concurrent malignancy or severe chronic consumptive disease; (6) loss to clinical follow-up; (7) suboptimal imaging quality or incomplete medical records; and (8) age younger than 18 years at enrollment.

For the non-PPDM-A control cohort, enrollment required a confirmed diagnosis of acute pancreatitis along with the following inclusion criteria: (1) complete clinical admission data available at initial acute pancreatitis onset; and (2) sustained normal glycemic parameters verified by systematic medical record review and follow-up telephone interviews through May 2025. Exclusion criteria for the control group were: (1) acute exacerbation of chronic pancreatitis; (2) concomitant malignancy or severe chronic consumptive disease; (3) secondary complications related to congenital or acquired pancreatic anatomical abnormalities; (4) loss to follow-up; and (5) suboptimal imaging quality or incomplete clinical documentation.

CT technical details were as follows. All enrolled patients underwent abdominal contrast-enhanced CT using 1 of 3 multidetector-row CT systems: Aquilion ONE (Toshiba, Tokyo, Japan), Ingenuity CT (Philips Medical Systems), or Somatom Definition Flash (Siemens Healthineers). For the Aquilion ONE and Ingenuity CT scanners, standardized acquisition parameters were as follows: tube voltage, 120 kV; tube current, 250 mA; field of view, 40 × 40 cm; matrix size, 512 × 512; slice thickness, 5.0 mm; collimation, 320 × 0.5 mm with automatic reconstruction; and pitch values of 0.87 and 1.015, respectively. After routine unenhanced abdominal scanning, arterial- and portal venous-phase images were acquired at 25 to 30 seconds and 48 to 50 seconds after contrast injection. Iodinated contrast medium (Ultravist 370, Bayer Schering Pharma) was administered intravenously at a dose of 1.5 mL/kg and an injection rate of 3 mL/s using a power injector. For the Somatom Definition Flash scanner, acquisition parameters were as follows: tube voltage, 100 kV; tube current, 318 mA; field of view, 33 × 33 cm; collimation, 128 × 0.6 mm; pitch, 0.8; and slice thickness, 5.0 mm. Automatic exposure modulation (Care Dose 4D; Siemens Medical Solutions) was applied throughout scanning. After unenhanced baseline acquisition, arterial- and portal venous-phase contrast-enhanced CT images were obtained at 25 seconds and 40 seconds after contrast administration, respectively. The same iodinated contrast agent (Ultravist 370, Bayer Schering Pharma) was administered at a dose of 1.5 mL/kg, with an injection rate of 3.5 to 5 mL/s using a power injector.

All enrolled patients had plasma samples collected within 1 week after admission after acute pancreatitis onset. Plasma samples for proteomic analysis were stored at -80°C. Admission data were obtained from the hospital information system and included sex, age, RAC, EPIC, etiology, CTSI, presence or absence of pancreatic necrosis, recurrence status, and smoking history. Two abdominal radiologists with at least 5 years of experience independently reviewed the CT scans and calculated the CTSI [26], RAC [21], and EPIC scores [27] while blinded to patient outcomes. Any discrepancies were resolved via consensus discussion. Due to incomplete data, metabolic variables were unavailable for analysis.

Follow-up periods were defined as follows: for patients with PPDM-A, the follow-up period extended from the date of first discharge after acute pancreatitis to the date of diabetes mellitus diagnosis; for patients with PPNG-A, the follow-up period extended from the date of first discharge after acute pancreatitis until completion of observation (ie, July 2025).

This retrospective single-center study was approved by the Institutional Review Board of North Sichuan Medical College (ethical approval number: 202151), and the requirement for informed consent was waived. The study was conducted in accordance with the Declaration of Helsinki.

Proteomics Analysis

Protein Extraction and Peptide Enzymatic Digestion

Proteins were extracted from human plasma using SDT lysis buffer (100 mM Tris-HCl, 4% sodium dodecyl sulfate, pH 7.6). Protein concentrations were quantified via the bicinchoninic acid assay. For sodium dodecyl sulfate-polyacrylamide gel electrophoresis analysis, 20 µg of protein from each sample were mixed with an appropriate volume of 5 × loading buffer, heated in water for 5 minutes, and separated on a 4% to 20% precast gradient gel at a constant voltage of 180 V for 45 minutes, then subjected to Coomassie Brilliant Blue R-250 staining.

All samples were treated with dithiothreitol to reduce disulfide bonds and incubated at room temperature for 1 hours. Free thiol groups were blocked with iodoacetamide by incubation in the dark at room temperature for 30 minutes. Samples were then digested overnight with trypsin. The resulting peptides were desalted using a C18 cartridge, freeze-dried, and reconstituted in 40 µL of 0.1% formic acid. Peptide concentrations were determined by measuring optical density at 280 nm. Digested peptides from each sample were mixed with an appropriate amount of indexed retention time standard peptides for DIA mass spectrometry.

The proteomics operator was blinded to patient outcomes; they applied random batch allocation and randomized sample testing order. All experiments were performed in triplicate, and average values were used for analysis.

Indexed in: [Current Contents/Clinical Medicine] [SCI Expanded] [ISI Alerting System] [ISI Journals Master List] [Index Medicus/MEDLINE] [EMBASE/Excerpta Medica] [Chemical Abstracts/CAS]

Mass Spectrometry

DIA analysis for chromatographic separation was performed via the Evosep One system with a nanoliter flow rate. Samples separated by nanoliter high-performance liquid chromatography were analyzed using a Bruker timsTOF mass spectrometer in DIA mode. Mass spectrometry and tandem mass spectrometry data were acquired in positive ion mode. The mass spectrometry scanning range was 100 to 1700 m/z. MS2 acquisition included 4 trapped ion mobility spectrometry scan windows with a total cycle time of 100 ms using DIA acquisition mode. In parallel accumulation-serial fragmentation mode, collision energy varied linearly according to ion mobility $1/K_0$; fragmentation energies ranging from 20 to 59 eV corresponded to ion mobility values of $1/K_0 = 0.85$ to 1.30 Vs/cm^2.

Data Analysis

DIA data were processed via Spectronaut 19 software. Dynamic indexed retention time was selected for retention time prediction, and interference correction at the MS2 level was enabled. Carbamidomethylation was set as a fixed modification; acetylation (protein N-terminus) and oxidation were regarded as dynamic modifications. A maximum of 2 missed cleavage sites was allowed, and cross-run normalization was enabled. All data passed a Q-value threshold of 0.01 (false discovery rate < 1%). Differentially expressed proteins were defined using an adjusted P value < 0.05.

Bioinformatics Analysis Methods

Protein clustering analysis: Quantitative data for the target protein set were first standardized to the interval (-1, 1). Hierarchical clustering heatmaps were generated via the ComplexHeatmap R package (R version 3.6.1) by simultaneously clustering samples and protein expression profiles in 2 dimensions (linkage method: average linkage; distance metric: Euclidean distance). Normalized target protein data were then analyzed using the fuzzy c-means algorithm implemented in the Mfuzz software package. Expression trends were classified into distinct expression modules to identify different clustering patterns.

Subcellular localization analysis: Multiclass support-vector-machine-based machine learning models were used to analyze available subcellular localization data for the identified proteins via sequence-based modeling. Subcellular localization was predicted using CELLO (http://cello.life.nctu.edu.tw/). This method was utilized to predict the subcellular localization of all identified proteins.

Kyoto Encyclopedia of Genes and Genomes (KEGG) pathway annotation: For the target protein set, KEGG pathway annotation was performed using KOBAS 3.0.

Enrichment analysis: Pathway distributions were compared between the target protein set and the overall protein set via Fisher's exact test, followed by KEGG pathway enrichment analysis of the target protein set.

Enzyme-Linked Immunosorbent Assay (ELISA)

Plasma levels of complement factor I (CFI), coagulation factor XII (F12), and immunoglobulin heavy chain (IgH) in patients with PPDM-A or PPNG-A were measured using commercial double-antibody ELISA kits (Chongqing Bonoheng Biotechnology, Chongqing, China; catalog numbers: BNH-070421H, BNH-161694H, and BNH-090718H, respectively). All assays were performed in accordance with the manufacturer's instructions.

The ELISA operator was blinded to patient outcomes; they applied random batch allocation and randomized sample testing order. All experiments were performed in triplicate, and average values were used for analysis.

Statistical Analysis

PASS 21.0.3 for Windows (NCSS, Kaysville, UT, USA) was used for sample size estimation. Statistical analyses were performed with SPSS 22.0 for Windows (IBM, Armonk, NY, USA). Data normality for each group was assessed via the Shapiro-Wilk test. Continuous variables with approximately normal distributions are presented as mean ± standard deviation; continuous variables with non-normal distributions are presented as median (interquartile range). Continuous variables were compared using either the independent-samples t-test or the Mann-Whitney U test, as appropriate. Categorical variables were compared using the chi-square test or Fisher's exact test. Correlations between target proteins and acute pancreatitis severity were assessed via Pearson or Spearman correlation analysis. Receiver operating characteristic (ROC) curve analysis was performed to evaluate the diagnostic performance of acute pancreatitis severity scores and target proteins for predicting PPDM-A. Area under the ROC curve (AUC) values were compared using the DeLong test performed by GraphPad Prism (version 10.2.3, GraphPad, La Jolla, CA, USA). All statistical tests were 2-tailed, and $P < 0.05$ was considered statistically significant.

Results

Demographic Characteristics

Plasma samples from 65 patients with acute pancreatitis were collected at admission. Of these patients, 18 were lost to follow-up, 17 had a previous diagnosis of type 2 diabetes mellitus, 7 lacked post-discharge blood glucose data, 2 died, and 1 had lung cancer. One plasma sample was contaminated during

Indexed in: [Current Contents/Clinical Medicine] [SCI Expanded] [ISI Alerting System] [ISI Journals Master List] [Index Medicus/MEDLINE] [EMBASE/Excerpta Medica] [Chemical Abstracts/CAS]

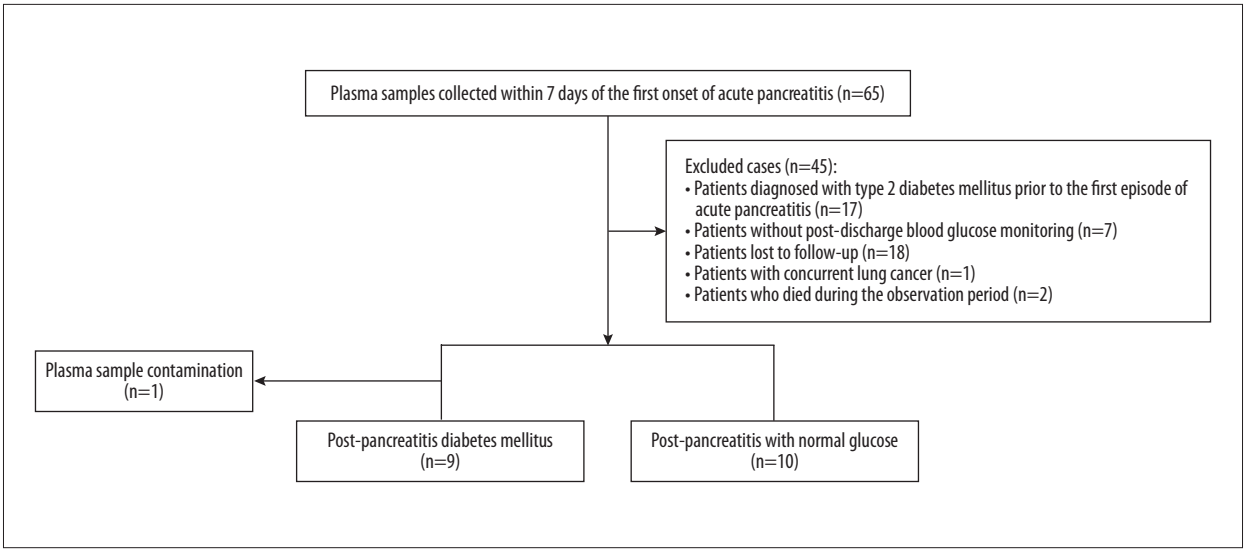

Figure 1. Flowchart of patient recruitment in this study.

experimentation. Ultimately, 9 patients with PPDM-A and 10 patients with PPNG-A—matched for age, sex, and etiology—were included in the analysis. The patient recruitment flowchart is shown in **Figure 1**.

Sample size calculations indicated that the final cohort of 19 patients met the minimum sample size required for statistical significance (see the **Sample Size Estimation** section below for details).

The PPDM-A group had a significantly higher incidence of pancreatic necrosis compared with the PPNG-A group ($P = 0.047$). No significant differences between groups were observed concerning age, CTSI, etiology, sex, EPIC score, follow-up duration, RAC, smoking status, or recurrence status (**Table 1**). Representative CT images are shown in **Figure 2**.

PPDM-A Diagnosis

Diagnostic criteria for PPDM-A were as follows: (I) fasting plasma glucose of at least 126 mg/dL (7.0 mmol/L), 3 patients; (II) 2-h plasma glucose of at least 11.1 mmol/L after a 75-g oral glucose tolerance test, 3 patients; (III) random blood glucose of at least 200 mg/dL (11.1 mmol/L) accompanied by diabetic symptoms, 1 patient; and (IV) glycated hemoglobin of at least 6.5% (48 mmol/mol), 2 patients. The median interval from the initial acute pancreatitis episode to diabetes mellitus diagnosis was 19 months (interquartile range: 13.50-20.00 months). Diagnoses were confirmed via telephone follow-up and repeat blood glucose testing at readmission. None of the 9 patients had received antidiabetic treatment before diagnosis.

Proteomics Analysis

The DIA proteomics approach was used to evaluate plasma samples from the PPNG-A and PPDM-A groups. In total, 90 differentially expressed proteins (fold change > 1.2 or < 0.8, $P < 0.05$) were identified between the 2 groups. Among these proteins, 64 were localized extracellularly, 21 in the nucleus, 2 each in the cell membrane and cytoplasm, and 1 in the mitochondrion (**Figure 3A**). Compared with the PPNG-A group, the PPDM-A group exhibited 56 downregulated and 34 upregulated differentially expressed proteins. Details are shown in the volcano plot of differential protein expression (**Figure 3B**). A normalized hierarchical clustering heatmap of the 90 differentially expressed proteins clearly distinguished PPDM-A samples from PPNG-A samples (**Figure 3C**). To further investigate signaling pathways associated with PPDM-A, KEGG enrichment analysis was performed on the differentially expressed proteins. The top 20 enriched KEGG pathways are presented in **Figure 3D**. This study focused on 3 pathways associated with acute pancreatitis: NF-κB signaling, complement-coagulation cascades, and calcium signaling. Nine proteins were identified in complement-coagulation cascades, 4 in the NF-κB signaling pathway, and 4 in the calcium signaling pathway. Among these proteins, CFI, F12, and IgH showed the most pronounced differential expression. CFI and F12 are involved in complement-coagulation cascades, whereas IgH is associated with both the NF-κB and calcium signaling pathways. These proteins play important roles in immune and inflammatory responses. Compared with the PPNG-A group, the PPDM-A group showed upregulated CFI expression (1.752-fold increase). In contrast, F12 and IgH expression levels were downregulated (fold changes of 0.508 and 0.638, respectively; **Table 2, Figure 4**). Protein selection was based on pathway-driven and data-driven analyses.

Indexed in: [Current Contents/Clinical Medicine] [SCI Expanded] [ISI Alerting System] [ISI Journals Master List] [Index Medicus/MEDLINE] [EMBASE/Excerpta Medica] [Chemical Abstracts/CAS]

Table 1. Clinical characteristics of the PPDM-A and PPNG-A groups.

Clinical characteristics	PPDM-A (n = 9)	PPNG-A (n = 10)	*P*
Male sex	7 (77.78%)	6 (60.00%)	0.405
Age (years)	51.33 ± 12.4	58 ± 16.57	0.339
Etiology			0.553
Biliary	4 (44.44%)	4 (40.00%)	
Hyperlipidemia	4 (44.44%)	3 (30.00%)	
Alcohol consumption	1 (11.11%)	1 (10.00%)	
Specific pancreatitis	0	2 (20.00%)	
CT timing from symptom onset (days)	4 (2.5-3.5)	4 (3-6)	0.735
CTSI score	4 (2-6)	4 (2-4)	0.603
RAC			0.066
Mild	3 (33.33%)	2 (20%)	
Moderate to severe	3 (33.33%)	8 (80%)	
Severe	3 (33.33%)	0	
EPIC score	5 (1-7)	5 (0-6)	0.477
Follow-up duration (months)	19 (13.50-20.00)	20 (15.25-20.00)	0.328
Pancreatic necrosis			0.047*
No	6 (66.67%)	10 (100.00%)	
Yes	3 (33.33%)	0	
Recurrence			0.109
Yes	5 (55.56%)	2 (20.00%)	
No	4 (44.44%)	8 (80.00%)	
Smoking status			0.764
Yes	6 (66.67%)	6 (60.00%)	
No	3 (33.33%)	4 (40.00%)	

Note: Age approximately followed a normal distribution and is presented as mean ± standard deviation. CTSI, EPIC, and CT timing from symptom onset data showed skewed distributions and are presented as median (interquartile range). Sex, etiology, RAC, pancreatic necrosis, recurrence status, and smoking status are presented as frequencies (percentages). * $P < 0.05$. CT, computed tomography; CTSI, computed tomography severity index; EPIC, extrapancreatic inflammation on computed tomography score; PPDM-A, post-pancreatitis diabetes mellitus; PPNG-A, post-pancreatitis normal glucose; RAC, revised Atlanta classification.

ELISA

ELISA was used to measure plasma levels of CFI, F12, and IgH. The mean plasma CFI level was significantly higher in the PPDM-A group (376.144 ± 42.259 ng/mL) than in the PPNG-A group (216.900 ± 62.394 ng/mL; $P < 0.001$). Despite repeated ELISA experiments, F12 and IgH could not be reliably validated. Therefore, subsequent analyses involving F12 and IgH were based on relative proteomic expression values. CFI was considered the primary biomarker candidate; F12 and IgH were retained only as exploratory proteomic signals. Detailed results are presented as scatter plots in **Figure 5**.

Sample Size Estimation

Given that plasma expression levels of CFI, F12, and IgH in patients with PPDM-A or PPNG-A have not previously been reported, a pilot experiment was conducted to estimate the

Indexed in: [Current Contents/Clinical Medicine] [SCI Expanded] [ISI Alerting System] [ISI Journals Master List] [Index Medicus/MEDLINE] [EMBASE/Excerpta Medica] [Chemical Abstracts/CAS]

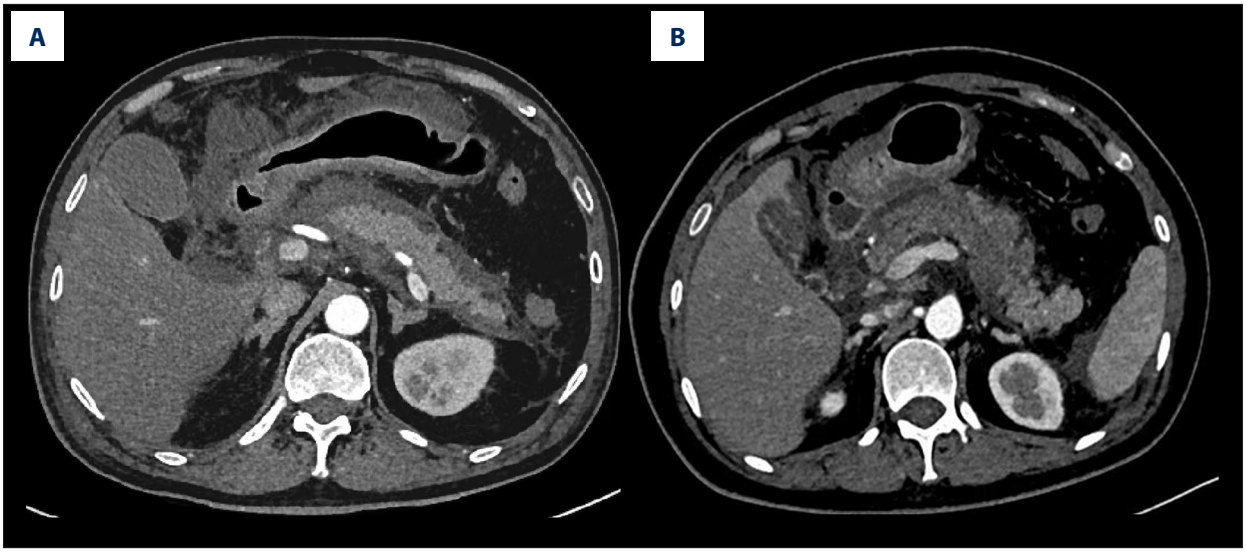

Figure 2. Representative CT images from 2 patients with acute pancreatitis. (**A**) CT image obtained at admission from a patient with moderate acute pancreatitis who did not develop diabetes mellitus during follow-up. CTSI = 4 and EPIC = 5. Pancreatic changes were limited to interstitial edema, and no pancreatic necrosis was observed. (**B**) CT image obtained at admission from a patient with moderate-to-severe acute pancreatitis who developed diabetes mellitus during follow-up. CTSI = 8 and EPIC = 7, with 30% to 50% pancreatic necrosis observed. CT, computed tomography; CTSI, computed tomography severity index; EPIC, extrapancreatic inflammation on CT score.

sample size based on proteomic and ELISA data. Specifically, ELISA data were used for CFI because it was successfully validated by ELISA; proteomic data were used for F12 and IgH because ELISA validation was unsuccessful. Sample size estimation showed that, considering 80% statistical power and a type I error rate of 5%, the minimum sample sizes required to detect statistically significant differences in protein expression between groups were 13 for CFI, 18 for IgH, and 19 for F12. Detailed results are presented in **Table 3**. Accordingly, the total sample size of 19 patients in the present study met the minimum statistical requirements. The sample size calculation was performed post hoc and applies only to the detection of observed biomarker differences, not to the development or validation of a prediction model.

Efficacies of CFI, F12, IgH, and Acute Pancreatitis Severity Scores for Predicting PPDM-A

Regarding discrimination of PPDM-A, the AUC values for CFI, F12, and IgH were 0.878, 0.856, and 0.867 respectively; there were no significant differences among the 3 markers ($P > 0.05$). When CFI, F12, and IgH were combined for discrimination analysis, the AUC increased to 0.989. However, this AUC was derived from the same discovery cohort and thus is likely to be optimistic. The combined biomarker model showed significantly higher discriminatory performance relative to CTSI, RAC, and EPIC scores (0.989 vs 0.578, $P = 0.005$). ROC curves evaluating the predictive performances of CFI, F12, and IgH for PPDM-A are shown in **Figure 6**.

Correlation Analysis of CFI, F12, IgH, and Acute Pancreatitis Severity Scores

F12 was significantly negatively correlated with CTSI and RAC scores ($P = 0.043$ and 0.035; R = -0.468 and -0.485, respectively), but not with the EPIC score ($P = 0.138$). CFI and IgH were not significantly correlated with CTSI, RAC, or EPIC scores (all $P > 0.05$) (**Table 4**).

Correlation Analysis of CFI, F12, and IgH With Imaging Features of Acute Pancreatitis (Pancreatic Necrosis)

CFI was significantly positively correlated with pancreatic necrosis ($P = 0.020$, R = 0.527); F12 was significantly negatively correlated with pancreatic necrosis ($P = 0.040$, R = -0.474). IgH was not correlated with pancreatic necrosis ($P = 0.668$, R = 0.105) (**Table 5**). Independence from pancreatic necrosis was not demonstrated.

Discussion

This study compared and analyzed the clinical characteristics, severity scores, and imaging features of patients with PPNG-A and those with PPDM-A upon admission for acute pancreatitis. The PPDM-A group showed a higher incidence of pancreatic necrosis relative to the PPNG-A group. However, no significant differences between groups were observed regarding CTSI, sex, etiology, age, EPIC score, RAC, follow-up duration,

Indexed in: [Current Contents/Clinical Medicine] [SCI Expanded] [ISI Alerting System] [ISI Journals Master List] [Index Medicus/MEDLINE] [EMBASE/Excerpta Medica] [Chemical Abstracts/CAS]

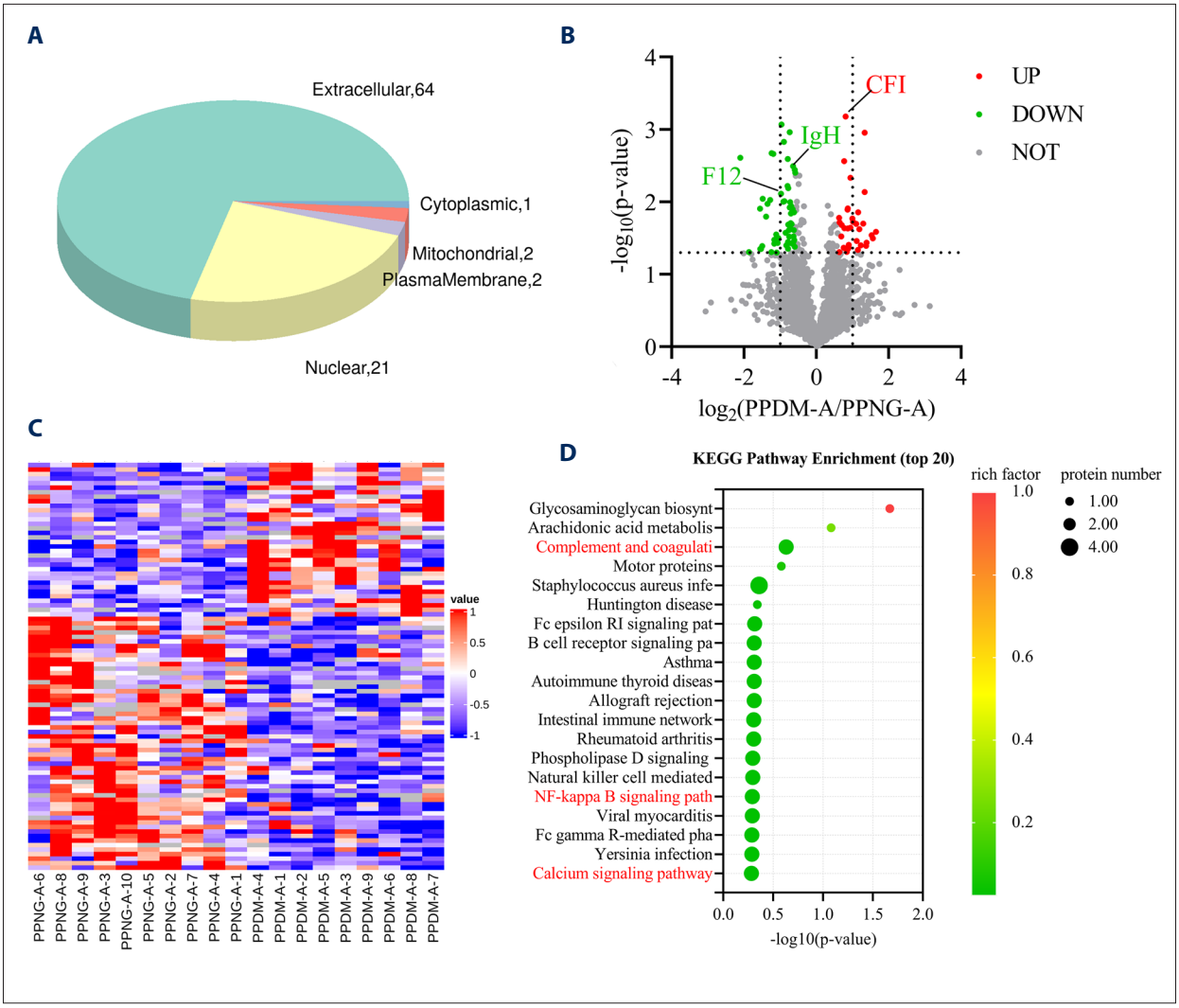

Figure 3. DIA proteomics analysis of patients with PPDM-A or PPNG-A. (**A**) Subcellular localization of DEPs. (**B**) Volcano plot showing DEPs between groups. Compared with the PPNG-A group, significantly upregulated DEPs in the PPDM-A group are shown in red, significantly downregulated DEPs are shown in blue, and proteins lacking significant expression differences are shown in gray. (**C**) Hierarchical clustering heatmap of DEPs in the PPDM-A and PPNG-A groups. Each column represents an individual sample, and each row represents a single DEP. Red indicates significantly upregulated proteins, blue indicates significantly downregulated proteins, and gray indicates proteins without valid quantitative data. (**D**) Bubble chart showing KEGG pathway enrichment analysis of all DEPs between the PPDM-A and PPNG-A groups. DEP, differentially expressed protein; DIA, data-independent acquisition; PPDM-A, post-pancreatitis diabetes mellitus; PPNG-A, post-pancreatitis normal glucose.

Table 2. Plasma levels of CFI, F12, and IgH in the PPDM-A and PPNG-A groups.

Proteins	PPDM-A	PPNG-A	PPDM-A/PPNG-A	P
CFI (ng/mL)	641.565 ± 186.84	366.169 ± 90.753	1.752	0.001*
F12	420.557 ± 281.307	828.564 ± 304.508	0.508	0.008*
IgH	2593.942 ± 1207.003	4065.145 ± 595.806	0.638	0.003*

Note: CFI was absolutely quantified in ng/mL, whereas IgH and F12 were relatively quantified using peak area integrals. CFI values shown here (from proteomics-based quantification) are distinct from ELISA-derived values in the main text. PPDM-A/PPNG-A represents the ratio of protein expression levels between groups. * $P < 0.05$. CFI, complement factor I; F12, coagulation factor XII; IgH, immunoglobulin heavy chain; PPDM-A, post-pancreatitis diabetes mellitus; PPNG-A, post-pancreatitis normal glucose.

Indexed in: [Current Contents/Clinical Medicine] [SCI Expanded] [ISI Alerting System] [ISI Journals Master List] [Index Medicus/MEDLINE] [EMBASE/Excerpta Medica] [Chemical Abstracts/CAS]

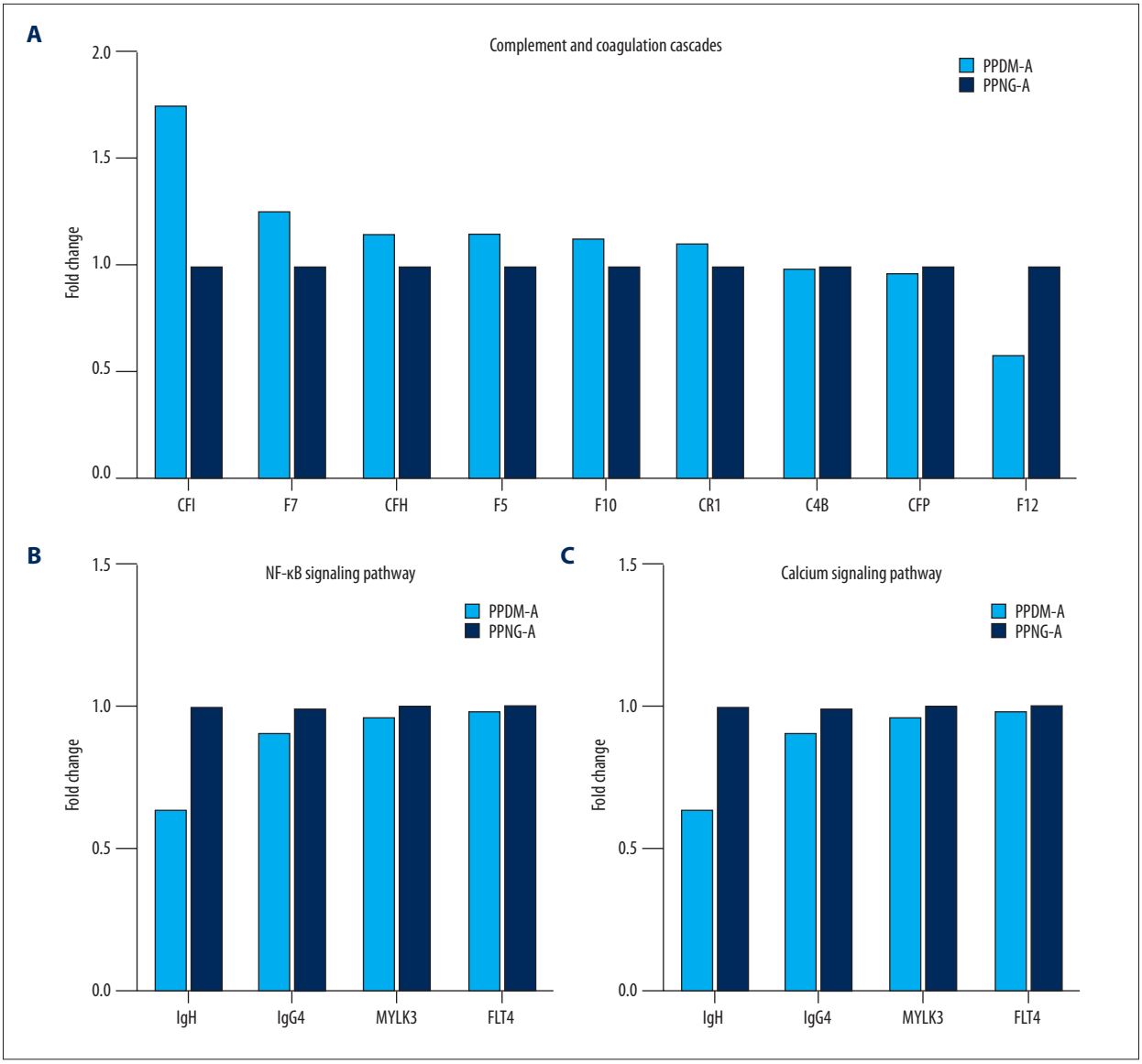

Figure 4. Fold changes in differential protein expression within the corresponding signaling pathways. (**A**) Fold changes in CFI and F12 expression relative to other proteins in complement and coagulation cascades. (**B, C**) Fold changes in IgH expression relative to other proteins in the NF-κB and calcium signaling pathways. CFI, complement factor I; F12, coagulation factor XII; IgH, immunoglobulin heavy chain; NF-κB, nuclear factor-κB; PPDM-A, post-pancreatitis diabetes mellitus; PPNG-A, post-pancreatitis normal glucose.

recurrence status, smoking status, or alcohol consumption. These findings suggest that radiologists should pay particular attention to pancreatic necrosis when evaluating patients with pancreatitis—it may indicate the potential development of PPDM-A and an increased risk of adverse complications.

Proteomic analysis was subsequently used to compare plasma protein profiles at admission between patients with PPDM-A and those with PPNG-A during acute pancreatitis. To our knowledge, this study is the first to show that plasma CFI levels were increased in the PPDM-A group, whereas F12 and IgH levels were decreased, compared with the PPNG-A group. Notably, CFI and F12 are involved in complement-coagulation cascades; IgH is associated with both the NF-κB and calcium signaling pathways. Combined discriminatory analysis using CFI, F12, and IgH yielded an AUC of 0.989. However, this result was derived from the same discovery cohort and should be interpreted cautiously. Additionally, although CFI and F12 were associated with pancreatic necrosis, they did not exhibit independence from pancreatic necrosis. These proteins may also reflect broader pathophysiological processes, including islet cell injury and inflammatory amplification [14,28], beyond CT-based severity assessment.

Indexed in: [Current Contents/Clinical Medicine] [SCI Expanded] [ISI Alerting System] [ISI Journals Master List] [Index Medicus/MEDLINE] [EMBASE/Excerpta Medica] [Chemical Abstracts/CAS]

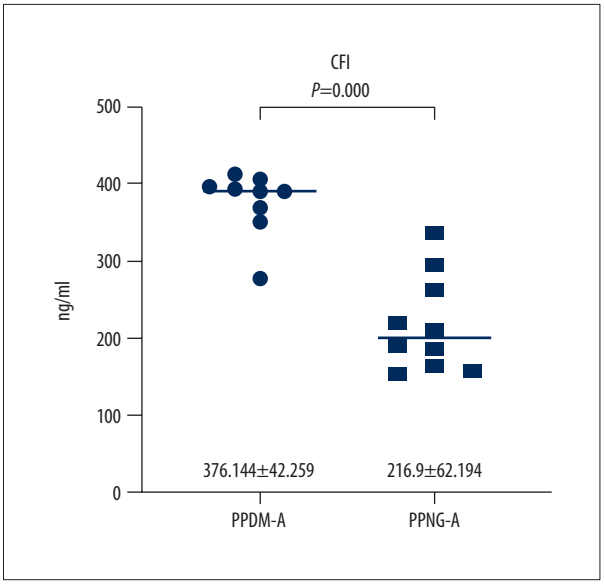

Figure 5. Plasma CFI levels in patients with PPDM-A or PPNG-A. CFI, complement factor I; PPDM-A, post-pancreatitis diabetes mellitus; PPNG-A, post-pancreatitis normal glucose.

Our study demonstrated that plasma CFI levels were significantly increased in patients with PPDM-A, and this finding was successfully validated by ELISA, suggesting that CFI overexpression is associated with the development of PPDM-A. Previous research by Zhang et al identified elevated serum CFI levels in necrotizing acute pancreatitis, indicating an association between CFI and acute pancreatic necrosis [14]. The authors suggested that pancreatic necrosis can trigger complement-coagulation cascades, thereby exacerbating pancreatitis severity and inflammatory responses. In the present study, CT imaging showed a lower incidence of pancreatic necrosis in the PPNG-A group than in the PPDM-A group; CFI levels were significantly positively correlated with pancreatic necrosis. These findings provide a molecular explanation for the observed imaging characteristics and suggest that when pancreatic necrosis is detected on CT, plasma CFI levels should be assessed because elevated CFI may indicate an increased risk of PPDM-A. Given that destruction of pancreatic islet cells after pancreatic necrosis contributes to diabetes mellitus onset [8,9], in conjunction with existing evidence, we hypothesize that elevated CFI levels are associated with the necrotic process in acute pancreatitis and may reflect mechanisms linked to pancreatic necrosis and subsequent diabetes mellitus risk. However, no direct mechanistic experiments were performed in the present study to establish causal relationships.

Plasma F12 levels were decreased in patients with PPDM-A. As a coagulation factor, F12 is primarily synthesized in the liver and plays a key role in endogenous coagulation. The pathogenesis of acute pancreatitis is complex, involving interactions between inflammatory mediators and coagulation factors [28]. Inflammatory mediators such as interleukins and tumor necrosis factor can activate the coagulation system and promote thrombin generation, thereby enhancing coagulation and amplifying inflammation [29,30]. Additionally, excessive activation of the coagulation system can lead to microvascular thrombosis, resulting in pancreatic microcirculatory dysfunction, impaired islet cell function, and disrupted insulin secretion [31]. During acute pancreatitis, coagulation imbalance may produce a hypercoagulable state, leading to consumption of coagulation factors such as F12, accumulation of fibrin degradation products, worsening pancreatic microcirculatory disturbance, intensified inflammatory responses, and aggravated pancreatic injury; such factors may ultimately contribute to diabetes mellitus development [14,31]. Based on these observational associations and previous literature, we speculate that reduced plasma F12 levels in patients with PPDM-A

Table 3. Sample size estimation.

Proteins	Target power	Actual power	N1	N2	N	μ1	μ2	δ	σ1	σ2	Alpha
CFI	0.8	0.979	3	10	13	376	217	159	42	62	0.05
F12	0.8	0.816	9	10	19	421	829	-408	281	305	0.05
IgH	0.8	0.808	8	10	18	2594	4065	-1471	1207	596	0.05

Note: The hypotheses for the test were as follows: H0: $\delta = 0$, indicating no difference between the population means of the groups; H1: $\delta \neq 0$, indicating a difference between the population means of the groups. $\delta = \mu1 - \mu2$ represents the difference between the population means, where μ1 and μ2 are the hypothesized population means. Target power refers to the desired power level specified in PASS software; actual power refers to the power obtained under current conditions. Statistical power represents the probability of rejecting a false null hypothesis. N1 and N2 represent the sample sizes of the PPDM-A and PPNG-A groups, respectively, and N = N1 + N2 represents the total sample size. σ1 and σ2 represent the hypothesized population standard deviations of the PPDM-A and PPNG-A groups, respectively. Alpha represents the probability of rejecting a true null hypothesis and was set at 0.05, corresponding to a type I error rate of 5%. CFI, complement factor I; F12, coagulation factor XII; IgH, immunoglobulin heavy chain.

Indexed in: [Current Contents/Clinical Medicine] [SCI Expanded] [ISI Alerting System] [ISI Journals Master List] [Index Medicus/MEDLINE] [EMBASE/Excerpta Medica] [Chemical Abstracts/CAS]

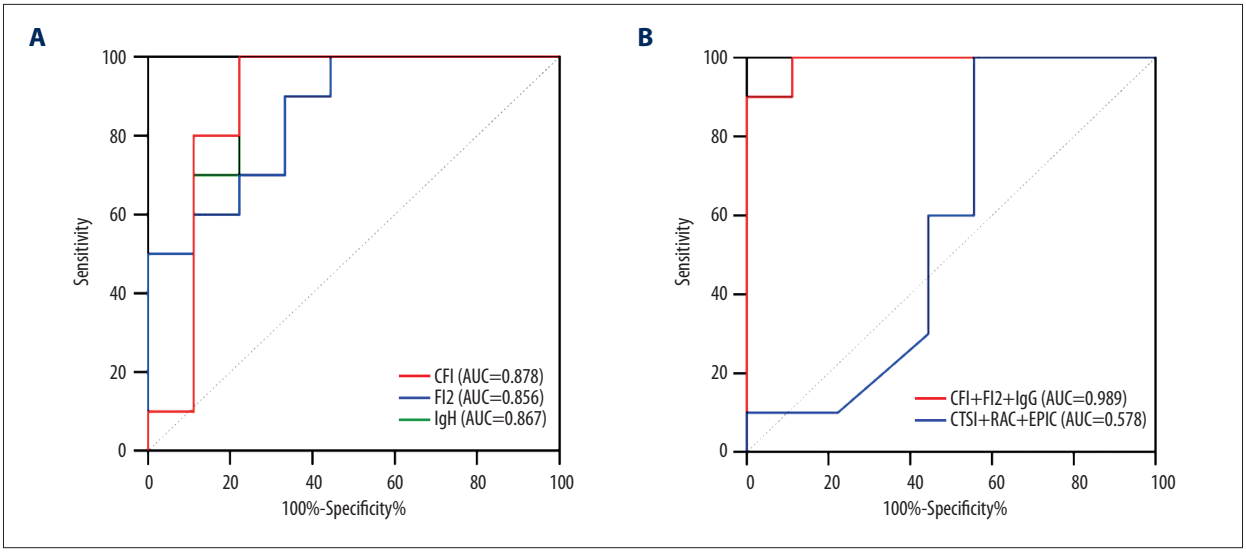

Figure 6. ROC curves for predicting PPDM-A using CFI, F12, IgH, and acute pancreatitis severity scores. (**A**) ROC curves for the individual prediction of PPDM-A using CFI, F12, and IgH. (**B**) ROC curves comparing the combined biomarker model (CFI+F12+IgH) with the combined imaging severity score model (CTSI+RAC+EPIC) for PPDM-A prediction. AUC, area under the receiver operating characteristic curve; CTSI, computed tomography severity index; EPIC, extrapancreatic inflammation on computed tomography; PPDM-A, post-pancreatitis diabetes mellitus; RAC, revised Atlanta classification; ROC, receiver operating characteristic curve.

Table 4. Correlation analysis of CFI, F12, and IgH with acute pancreatitis severity scores.

Proteins	Acute pancreatitis severity scores	Correlation coefficient	*P*
CFI	CTSI	0.355	0.135
CFI	EPIC	0.003	0.992
CFI	RAC	-0.202	0.407
F12	CTSI	-0.468	0.043*
F12	EPIC	-0.353	0.138
F12	RAC	-0.485	0.035*
IgH	CTSI	0.229	0.345
IgH	EPIC	0.273	0.259
IgH	RAC	0.237	0.328

Note: * $P < 0.05$. CFI, complement factor I; CTSI, computed tomography severity index; EPIC, extrapancreatic inflammation on computed tomography score; F12, coagulation factor XII; IgH, immunoglobulin heavy chain; RAC, revised Atlanta classification.

Table 5. Correlation analysis of CFI, F12, and IgH with imaging features of acute pancreatitis (pancreatic necrosis).

Proteins	Imaging features of acute pancreatitis	Correlation coefficient	*P*
CFI	Pancreatic necrosis	0.527	0.02*
F12	Pancreatic necrosis	-0.474	0.04*
IgH	Pancreatic necrosis	0.105	0.668

Note: * $P < 0.05$. CFI, complement factor I; F12, coagulation factor XII; IgH, immunoglobulin heavy chain.

Indexed in: [Current Contents/Clinical Medicine] [SCI Expanded] [ISI Alerting System] [ISI Journals Master List] [Index Medicus/MEDLINE] [EMBASE/Excerpta Medica] [Chemical Abstracts/CAS]

reflect activation and consumption of the coagulation system. However, no mechanistic experiments were performed to validate this proposed pathway. As acute pancreatitis severity increases, plasma F12 levels may progressively decline, potentially reflecting excessive coagulation activation, worsening pancreatic microcirculatory dysfunction, and impaired islet cell function, thus contributing to diabetes mellitus development. Intriguingly, F12 was negatively correlated with pancreatic necrosis. Collectively, CFI and F12 may represent candidate biomarkers reflecting necrosis-associated inflammatory and coagulation processes linked to subsequent PPDM-A. The underlying molecular mechanisms warrant further investigation in future functional studies.

IgH has multiple biological functions. Our study revealed that IgH is associated with both calcium signaling and NF-κB pathways; to our knowledge, this is the first study to show significant downregulation of plasma IgH in patients with PPDM-A. These findings provide preliminary evidence to support a potential role for IgH in PPDM-A pathogenesis. Calcium overload in pancreatic acinar cells is a key trigger of acute pancreatitis [32]. Physiological calcium signaling is essential for normal pancreatic digestive enzyme secretion. However, the pancreas is highly susceptible to stress-related dysregulation, which can cause excessive calcium release and lead to pathological changes, including abnormal intracellular enzyme activation and cellular vacuolization [33,34]. Based on these observations, we cautiously speculate that IgH downregulation disrupts calcium homeostasis through effects on calcium transport or regulatory mechanisms, potentially contributing to calcium overload and downstream pathophysiological changes relevant to islet cell injury. However, no direct mechanistic evidence was obtained in the present study to support this proposed pathway. NF-κB is a key transcription factor involved in immune regulation, apoptosis, inflammatory responses, and cell proliferation. NF-κB expression is elevated in acute pancreatitis and contributes to disease progression along with other inflammatory mediators [35,36]. We also speculate that reduced IgH expression is associated with abnormal activation of the NF-κB signaling pathway, potentially exacerbating inflammatory responses and cellular injury and impairing insulin secretion, thus contributing to PPDM-A development. These mechanistic interpretations are based on observational proteomic findings and existing literature, rather than direct experimental validation. The precise molecular mechanisms through which IgH regulates calcium signaling and NF-κB pathways in PPDM-A require further investigation through in vitro and in vivo methods. Notably, IgH is a core secretory molecule of B lymphocytes, which have been implicated in the pathophysiological progression of PPDM-A [15]. This evidence further supports the potential involvement of IgH in PPDM-A onset and progression. To date, research concerning the immune profiling of PPDM-A remains limited. Relatively few studies have explored associations between immune cell subsets, such as B lymphocytes [15], and PPDM-A prognosis; there is a lack of systematic investigation involving immune landscapes, immune-related molecular markers, and their regulatory mechanisms. By identifying IgH as an immune-related differentially expressed protein linked to immune-inflammatory signaling pathways, our study provides a novel perspective for the early prediction of PPDM-A and establishes a preliminary experimental basis to guide future studies investigating immune-mediated pathogenic mechanisms in PPDM-A.

We acknowledge that the AUC of 0.989 observed in this small exploratory cohort may be susceptible to overfitting due to the limited sample size and low events-per-variable ratio; therefore, this predictive performance should be interpreted cautiously. Nevertheless, the high AUC may reflect not only statistical overfitting but also genuine biological differences between the PPDM-A and PPNG-A groups. CFI, F12, and IgH were identified through DIA proteomics combined with KEGG enrichment analysis of pathways associated with acute pancreatitis pathogenesis, rather than through a single statistical screening approach. Among these proteins, IgH is an important immune-related molecule that may link immune dysregulation to PPDM-A pathogenesis, thus contributing to the current understanding of PPDM-A molecular mechanisms in the context of limited research on PPDM-A immune profiling. Complement-coagulation cascades play a central role in necrotizing pancreatitis, and pancreatic necrosis is a well-established mechanism underlying PPDM-A. Additionally, persistent inflammation is closely associated with islet β-cell dysfunction and PPDM-A development. Therefore, these molecules may contribute to PPDM-A pathogenesis through mechanisms related to pancreatic necrosis and inflammatory injury. Given the significant difference in pancreatic necrosis between groups ($P = 0.047$) and the correlations between CFI/F12 and pancreatic necrosis, we acknowledge that these markers may partially reflect the severity of tissue injury. As key molecules involved in pancreatic necrosis, inflammation, and islet β-cell dysfunction, CFI and F12 may also have broader biological and pathogenic relevance beyond serving solely as surrogate markers of pancreatic necrosis [14,28]. All mechanistic interpretations in this study are based on observational associations and published literature; no functional or mechanistic experiments were performed to establish causal relationships. Because these markers were selected according to pathophysiological mechanisms rather than on the basis of their correlations with pancreatic necrosis, they may still provide independent predictive value for PPDM-A. However, the present study did not include formal analyses of incremental predictive value beyond existing PPDM-A predictors.

Several limitations of this research should be acknowledged. First, although the sample size met the minimum requirement

Indexed in: [Current Contents/Clinical Medicine] [SCI Expanded] [ISI Alerting System] [ISI Journals Master List] [Index Medicus/MEDLINE] [EMBASE/Excerpta Medica] [Chemical Abstracts/CAS]

based on sample size estimation, the present work used a single-center design and relatively small cohort. As a long-term complication of acute pancreatitis, PPDM-A is frequently overlooked or misdiagnosed as type 2 diabetes mellitus, resulting in a limited number of eligible patients. Furthermore, information about metabolic variables was unavailable. Second, internal validation methods, such as cross-validation or bootstrapping, were not performed. This limitation may have increased the risk of overfitting and optimism bias, thereby reducing the reliability of reported AUC values. Third, although CFI and F12 are biologically plausible predictors of PPDM-A, their correlations with pancreatic necrosis imply that they may partially reflect tissue injury severity rather than providing fully independent predictive value. Fourth, baseline metabolic risk factors (eg, body mass index and family history of diabetes mellitus) were unavailable and thus could not be included in the analysis, representing potential confounders. Additionally, among the 3 differentially expressed proteins identified by proteomics (CFI, F12, and IgH), only CFI was successfully validated by ELISA. Repeated validation experiments for F12 and IgH produced unsatisfactory results. Future studies should validate these markers using alternative ELISA kits or other approaches, such as parallel reaction monitoring. Fifth, the median follow-up duration was 19 to 20 months. Although this duration substantially exceeded the minimum 3-month diagnostic window for PPDM-A and strict diagnostic criteria were utilized to minimize outcome misclassification, delayed onset of PPDM-A after the follow-up period could have resulted in false-negative classifications. Finally, due to the limited sample size, radiomic features were not analyzed in the present study. Future multicenter studies with larger cohorts are needed to integrate radiomics and proteomics in the development of a more robust multi-omics prediction model for PPDM-A.

Conclusions

This exploratory study demonstrated that plasma CFI levels were increased in the PPDM-A group, whereas F12 and IgH levels were significantly decreased, suggesting predictive value for PPDM-A. Moreover, CFI and F12 were significantly correlated with pancreatic necrosis (a CT imaging feature), thus linking plasma molecular alterations with imaging manifestations and providing a potential molecular explanation for the imaging characteristics of PPDM-A. These findings indicate that plasma biomarkers could reflect pathological changes associated with PPDM-A and may complement imaging features for early risk discrimination. Accordingly, this study provides a preliminary experimental basis for the early screening of PPDM-A and has identified hypothesis-generating biomarker candidates for future validation studies. Among the identified markers, CFI represents the strongest candidate because it was successfully validated by ELISA. In contrast, F12 and IgH remain exploratory biomarkers that require orthogonal validation before potential clinical application. Notably, the clinical utility of this diagnostic approach requires further confirmation in multicenter studies with larger sample sizes and both internal and external validation. Such analyses may provide more reliable evidence for the early and precise diagnosis and management of PPDM-A.

Availability of Data and Materials

The corresponding author can provide the data used in this study upon reasonable request. Raw and processed proteomics data are stored on the corresponding author's personal hard drive.

Declaration of Figures' Authenticity

All figures submitted have been created by the authors who confirm that the images are original with no duplication and have not been previously published in whole or in part.

References:

1. Cho J, Petrov MS. Epidemiology of post-pancreatitis diabetes mellitus: Insights from the COSMOS program. Expert Rev Endocrinol Metab. 2024;19(5):419-28
2. Olesen SS, Viggers R, Drewes AM, et al. Risk of major adverse cardiovascular events, severe hypoglycemia, and all-cause mortality in postpancreatitis diabetes mellitus versus type 2 diabetes: A nationwide population-based cohort study. Diabetes Care. 2022;45(6):1326-34
3. Cho J, Petrov MS. Pancreatitis, pancreatic cancer, and their metabolic sequelae: Projected burden to 2050. Clin Transl Gastroenterol. 2020;11(11):e00251
4. Charley E, Dinner B, Pham K, Vyas N. Diabetes as a consequence of acute pancreatitis. World J Gastroenterol. 2023;29(31):4736-43
5. Wynne K, Devereaux B, Dornhorst A. Diabetes of the exocrine pancreas. J Gastroenterol Hepatol. 2019;34(2):346-54
6. Cui Y, Andersen DK. Pancreatogenic diabetes: Special considerations for management. Pancreatology. 2011;11(3):279-94
7. Manrai M, Singh AK, Birda CL, et al. Diabetes mellitus as a consequence of acute severe pancreatitis: Unraveling the mystery. World J Diabetes. 2023;14(8):1212-25
8. Tu J, Zhang J, Ke L, et al. Endocrine and exocrine pancreatic insufficiency after acute pancreatitis: Long-term follow-up study. BMC Gastroenterol. 2017;17(1):114
9. Yu BJ, Li NS, He WH, et al. Pancreatic necrosis and severity are independent risk factors for pancreatic endocrine insufficiency after acute pancreatitis: A long-term follow-up study. World J Gastroenterol. 2020;26(23):3260-70
10. Zhi M, Zhu X, Lugea A, et al. Incidence of new onset diabetes mellitus secondary to acute pancreatitis: A systematic review and meta-analysis. Front Physiol. 2019;10:637
11. Pichardo-Lowden A, Goodarzi MO, Trikudanathan G, et al. Risk and factors determining diabetes after mild, nonnecrotizing acute pancreatitis. Curr Opin Gastroenterol. 2024;40(5):396-403

Indexed in: [Current Contents/Clinical Medicine] [SCI Expanded] [ISI Alerting System] [ISI Journals Master List] [Index Medicus/MEDLINE] [EMBASE/Excerpta Medica] [Chemical Abstracts/CAS]

12. Jakkampudi A, Jangala R, Reddy BR, et al. NF-κB in acute pancreatitis: Mechanisms and therapeutic potential. Pancreatology. 2016;16(4):477-88
13. Du W, Liu G, Shi N, et al. A microRNA checkpoint for Ca^{2+} signaling and overload in acute pancreatitis. Mol Ther. 2022;30(4):1754-74
14. Zhang X, Li Z, Liu W, et al. The complement and coagulation cascades pathway is associated with acute necrotizing pancreatitis by genomics and proteomics analysis. J Inflamm Res. 2022;15:2349-63
15. Lin X, Li X, Wang J, Liu H. B lymphocyte—A prognostic indicator in post-acute pancreatitis diabetes mellitus. J Diabetes. 2025;17(1):e70047
16. Williams KL, Gooley AA, Wilkins MR, Packer NH. A Sydney proteome story. J Proteomics. 2014;107:13-23
17. Ge P, Luo Y, Zhang G, Chen H. The role of proteomics in acute pancreatitis: New and old knowledge. Expert Rev Proteomics. 2024;21(1-3):115-23
18. Bourgault J, Abner E, Manikpurage HD, et al. Proteome-wide Mendelian randomization identifies causal links between blood proteins and acute pancreatitis. Gastroenterology. 2023;164(6):953-65.e953
19. Akshintala VS, Moore MG, Cruz-Monserrate Z, et al. Urine proteomics profiling identifies novel acute pancreatitis diagnostic biomarkers in a pediatric population. Gastroenterology. 2024;167(5):1019-21.e1012
20. Hu R, Yang H, Zeng GF, et al. A radiomics model of contrast-enhanced computed tomography for predicting post-acute pancreatitis diabetes mellitus. Quant Imaging Med Surg. 2024;14(3):2267-79
21. Banks PA, Bollen TL, Dervenis C, et al; Acute Pancreatitis Classification Working Group. Classification of acute pancreatitis—2012: Revision of the Atlanta classification and definitions by international consensus. Gut. 2013;62(1):102-11
22. American Diabetes Association Professional Practice Committee. 2. Classification and diagnosis of diabetes: Standards of medical care in diabetes—2022. Diabetes Care. 2022;45(Suppl. 1):S17-38
23. Petrov MS, Yadav D. Global epidemiology and holistic prevention of pancreatitis. Nat Rev Gastroenterol Hepatol. 2019;16(3):175-84
24. Petrov MS, Basina M. Diagnosing and classifying diabetes in diseases of the exocrine pancreas. Eur J Endocrinol. 2021;184(4):R151-63
25. Dugic A, Hagstrom H, Dahlman I, et al. Post-pancreatitis diabetes mellitus is common in chronic pancreatitis and is associated with adverse outcomes. United European Gastroenterol J. 2023;11(1):79-91
26. Alhajeri A, Erwin S. Acute pancreatitis: Value and impact of CT severity index. Abdom Imaging. 2008;33(1):18-20
27. De Waele JJ, Delrue L, Hoste EA, et al. Extrapancreatic inflammation on abdominal computed tomography as an early predictor of disease severity in acute pancreatitis: Evaluation of a new scoring system. Pancreas. 2007;34(2):185-90
28. Li L, Tan Q, Wu X, et al. Coagulopathy and acute pancreatitis: Pathophysiology and clinical treatment. Front Immunol. 2024;15:1477160
29. Kotan R, Peto K, Deak A, et al. Hemorheological and microcirculatory relations of acute pancreatitis. Metabolites. 2022;13(1):4
30. Greer PJ, Lee PJ, Paragomi P, et al. Severe acute pancreatitis exhibits distinct cytokine signatures and trajectories in humans: A prospective observational study. Am J Physiol Gastrointest Liver Physiol. 2022;323(5):G428-38
31. Jansson L, Carlsson PO. Pancreatic blood flow with special emphasis on blood perfusion of the islets of Langerhans. Compr Physiol. 2019;9(2):799-837
32. Pandol SJ, Gottlieb RA. Calcium, mitochondria and the initiation of acute pancreatitis. Pancreatology. 2022;22(7):838-45
33. Huang W, Booth DM, Cane MC, et al. Fatty acid ethyl ester synthase inhibition ameliorates ethanol-induced Ca^{2+}-dependent mitochondrial dysfunction and acute pancreatitis. Gut. 2014;63(8):1313-24
34. Criddle DN, Sutton R, Petersen OH. Role of Ca^{2+} in pancreatic cell death induced by alcohol metabolites. J Gastroenterol Hepatol. 2006;21(Suppl. 3):S14-17
35. Huang H, Liu Y, Daniluk J, et al. Activation of nuclear factor-κB in acinar cells increases the severity of pancreatitis in mice. Gastroenterology. 2013;144(1):202-10
36. Niu X, Sun W, Tang X, et al. Bufalin alleviates inflammatory response and oxidative stress in experimental severe acute pancreatitis through activating Keap1-Nrf2/HO-1 and inhibiting NF-κB pathways. Int Immunopharmacol. 2024;142(Pt A):113113

Indexed in: [Current Contents/Clinical Medicine] [SCI Expanded] [ISI Alerting System] [ISI Journals Master List] [Index Medicus/MEDLINE] [EMBASE/Excerpta Medica] [Chemical Abstracts/CAS]